Scientific Research Publishing

Journal of Modern Physics, 2026, 17(5), 679-696
https://www.scirp.org/journal/jmp
ISSN Online: 2153-120X
ISSN Print: 2153-1196

The Reality of Gravitational Repulsion, Its Impact in the Kerr Field and on Astrophysics

Charles H. McGruder III

Department of Physics and Astronomy, Western Kentucky University, Bowling Green, USA
Email: mcgruder@wku.edu

How to cite this paper: McGruder III, C.H. (2026) The Reality of Gravitational Repulsion, Its Impact in the Kerr Field and on Astrophysics. *Journal of Modern Physics*, **17**, 679-696.
https://doi.org/10.4236/jmp.2026.175029

Received: April 4, 2026
Accepted: May 24, 2026
Published: May 27, 2026

Abstract

Employing Boyer-Lindquist coordinates we show that the Kerr solution to the field equations of General Relativity leads to the conclusion that relativistic particles experience gravitational repulsion, $\frac{\mathrm{d}^2 r}{\mathrm{d}t^2} > 0$, in the weak-field regime, *i.e.*, as measured by distant observers. We consider only particles moving in axial motion or in the equatorial plane in the Kerr field. In both cases to the first order in weak fields relativistic particles experience gravitational acceleration, $\mathrm{d}^2 r/\mathrm{d}t^2 = +2g$, where $g = \frac{GM}{r^2}$. We reconcile the asymptotic result of McGruder (1982) and Krori & Barua (1985) with a systematic weak-field expansion, and identify higher-order Kerr corrections. The influence of rotation only becomes apparent in the second order. Implications for ultra-relativistic particles, ultra-high-energy cosmic rays, and compact astrophysical sources are discussed. After showing that gravitational repulsion exists in the Kerr field, we make it clear that gravitational repulsion corresponds to physical reality in both the Schwarzschild and Kerr fields.

Keywords

General Relativity, Kerr Metric, Gravitational Repulsion

1. Introduction

A substantial body of work has examined particle motion and acceleration in curved spacetimes, including both invariant and coordinate-dependent descriptions. Standard treatments of geodesic motion and observer dependence in General Relativity may be found in [1] [2]. Detailed analyses of particle trajectories and energy extraction processes in Kerr spacetimes have also been widely studied in astrophysical contexts [3]-[5]. These works provide the broader theoretical framework within which the present analysis may be situated.

As far back as 1916 it was discovered by [6] [7] and independently [8] [9] that a particle in radial motion will experience gravitational repulsion, $\frac{\mathrm{d}^2 r}{\mathrm{d}t^2} > 0$, in the Schwarzschild field, if its Schwarzschild velocity obeys the inequality:

$$\frac{\mathrm{d}r}{\mathrm{d}t} > \frac{1}{\sqrt{3}}\left(1 - \frac{\alpha}{r}\right) \tag{1}$$

where α is the Schwarzschild radius:

$$\alpha = 2GM \tag{2}$$

and where M is the mass of the gravitating body, G is the gravitational constant and the speed of light, $c = 1$. See [10] for the details of the history of this discovery.

After the discovery of gravitational repulsion decades of confusion and debate ensured. It was not until 1982 [11] that we were able to clarify the existence of gravitational repulsion in the Schwarzschild field. We applied our results to explain the acceleration of cosmic ray protons to ultra high energy via gravitational repulsion [12]. Next we used it to explain the acceleration of cosmic ray neutrinos to very high and ultra-high energy [13]. We also identified the type of sources that emit these particles. Also, we employed the theory to delinate the sources of very high and ultra-high energy cosmic ray protons [14].

All the above works assumed that the gravitational field of the sources are described by the Schwarzschild metric. Others discovered that gravitational repulsion exists in other metrics and other physical circumstances. Dickau, Kauffmann and Robertson employ it to solve the problem of the accelerating expansion of the universe (in preparation). [15] investigated gravitational repulsion in the Einstein-zero-mass scalar theory. [16] discussed gravitational repulsion in an expanding ball of dust. [17] considered gravitational repulsion in the Kerr-Newman anti-de Sitter spacetime. [18] examined into gravitational repulsion in the Reissner-Nordström and Schwarzschild spacetimes. [19] showed that the emission of gravitational waves leads to a repulsive gravitational force that diminishes with time but never disappears. They speculated that the repulsive force may be related to the observed expansion of the Universe. [20] pointed out that gravitational repulsion could appear in satellite experiments with beams of relativistic particles subject to very precise time measurements. [21] pointed out that gravitational repulsion occurs in geodesics in a quash-spherical spacetime. [22] investigated a number of aspects of the phenomenon of gravitational repulsion in static sources of the Reissner-Nordström field.

[23] studied gravitational repulsion in the Kerr and Kerr-Newman fields of black holes. Our work differs from their work in two major respects. Firstly, their work does not explicitly isolate the higher-order rotational contributions to the gravitational acceleration in expanded form.

Secondly, we emphasize that our results for gravitational repulsion in the Kerr field apply exactly to rotating black holes. However for rotating stars, brown dwarfs, and planetary bodies, the Kerr metric may serve as an approximation in appropriate regimes, but does not represent the exact exterior solution. This is important because in [13] we show that stellar mass bodies are the sources of ultra high energy neutrinos and in [14] we show that brown dwarfs are the sources of very high energy cosmic ray protons, while planetary mass bodies are the sources of the most energetic ultra high energy cosmic ray protons.

2. Gravitational Acceleration in the Kerr Field

We follow the approach of [11] to derive the gravitational acceleration in the Kerr field. The Kerr metric, Equation 3, describes the spacetime of a rotating gravitating source. The parameter a is defined as $a = \frac{J}{M}$ where J is the total angular momentum and M is the mass of the source (in units with $c = 1$). We express the Kerr metric in Boyer-Lindquist coordinates because in the limit $a \to 0$, these coordinates reduce to the Schwarzschild form, so that the motion in the two fields may be compared directly in terms of the same coordinate time t without ambiguity.

2.1. Asymptotic Interpretation and Conserved Energy

The Kerr spacetime is asymptotically flat. As $r \to \infty$, the metric reduces to Minkowski spacetime, whereby the coordinate time t becomes the proper time of inertial observers at infinity. The conserved quantity, $E = -p_t$, is therefore interpreted as the relativistic energy per unit rest mass measured by distant observers.

Specifically, the quantity E denotes the conserved energy per unit rest mass associated with the stationarity, that is time independence, of the Kerr field, $E = -p_t$. Its conservation does not contradict gravitational repulsion in the sense of [11]. The conserved quantity E refers to the particle's energy integral, whereas gravitational repulsion is determined by the sign of the radial acceleration with respect to the distant observer's time t. Thus a particle may have constant E and yet exhibit positive radial acceleration $\mathrm{d}^2 r/\mathrm{d}t^2 > 0$ for distant observers.

In the sense of [11], gravitational repulsion is defined with respect to the coordinate time t of distant observers, who are located in weak fields. Thus the sign of $\frac{\mathrm{d}^2 r}{\mathrm{d}t^2}$ determines whether the field is attractive or repulsive for such observers. If $\frac{\mathrm{d}^2 r}{\mathrm{d}t^2} > 0$, the field is repulsive for distant observers; if $\frac{\mathrm{d}^2 r}{\mathrm{d}t^2} < 0$ the field is attractive for distant observers.

2.2. Kerr Metric and Constants of Motion

The Kerr metric in Boyer-Lindquist coordinates is

$$\begin{aligned} \mathrm{d}s^2 = &-\left(1 - \frac{\alpha r}{\Sigma}\right)\mathrm{d}t^2 - \frac{2\alpha a r \sin^2\theta}{\Sigma}\mathrm{d}t\mathrm{d}\phi + \frac{\Sigma}{\Delta}\mathrm{d}r^2 + \Sigma \mathrm{d}\theta^2 \\ &+ \left(r^2 + a^2 + \frac{\alpha a^2 r \sin^2\theta}{\Sigma}\right)\sin^2\theta \mathrm{d}\phi^2, \end{aligned} \tag{3}$$

where

$$\Sigma = r^2 + a^2\cos^2\theta,\ \Delta = r^2 - \alpha r + a^2. \tag{4}$$

The quantities: $E = -p_t$, $L_z = p_\phi$ and Q are constants of motion of geodesics in the Kerr spacetime. Q is the Carter constant or Carter's constant of motion. It is an additional conserved quantity associated with motion in the polar direction. Setting $Q = 0$ restricts the motion to a plane. These are not parameters of the metric itself. Setting: $L_z = 0$ and $Q = 0$ does not alter the Kerr metric; it restricts the class of geodesics under consideration.

Moreover,

$$L_z = g_{\phi t}\frac{\mathrm{d}t}{\mathrm{d}\tau} + g_{\phi\phi}\frac{\mathrm{d}\phi}{\mathrm{d}\tau},$$

so that even when $L_z = 0$,

$$\frac{\mathrm{d}\phi}{\mathrm{d}\tau} = -\frac{g_{\phi t}}{g_{\phi\phi}}\frac{\mathrm{d}t}{\mathrm{d}\tau} \neq 0$$

in general. This is the effect of frame dragging. Only on the symmetry axis, where $g_{\phi t} = 0$, does one obtain the closest Kerr analogue of purely radial motion in the Schwarzschild field.

2.3. Axisymmetric Motion and Coordinate-Time Acceleration

In this section we restrict our attention to geodesics on the symmetry axis,

$$\theta = 0,\ L_z = 0,\ Q = 0.$$

Then

$$\Sigma = r^2 + a^2,\ \Delta = r^2 - \alpha r + a^2,$$

and the metric reduces to

$$\mathrm{d}s^2 = -\frac{\Delta}{r^2 + a^2}\mathrm{d}t^2 + \frac{r^2 + a^2}{\Delta}\mathrm{d}r^2. \tag{5}$$

2.3.1. Energy Integral

Using the geodesic Lagrangian

$$2\mathcal{L} = g_{\mu\nu}\frac{\mathrm{d}x^\mu}{\mathrm{d}\tau}\frac{\mathrm{d}x^\nu}{\mathrm{d}\tau}, \tag{6}$$

and Equation (5), we have

$$2\mathcal{L} = -\frac{\Delta}{r^2 + a^2}\left(\frac{\mathrm{d}t}{\mathrm{d}\tau}\right)^2 + \frac{r^2 + a^2}{\Delta}\left(\frac{\mathrm{d}r}{\mathrm{d}\tau}\right)^2. \tag{7}$$

Since the metric is independent of t, the conjugate momentum is conserved:

$$E = -p_t = -\frac{\partial\mathcal{L}}{\partial(\mathrm{d}t/\mathrm{d}\tau)} = \frac{\Delta}{r^2 + a^2}\frac{\mathrm{d}t}{\mathrm{d}\tau}. \tag{8}$$

Thus

$$\frac{\mathrm{d}t}{\mathrm{d}\tau} = \frac{E\left(r^2 + a^2\right)}{\Delta}. \tag{9}$$

2.3.2. Radial First Integral

The timelike normalization condition gives

$$g_{\mu\nu}\frac{\mathrm{d}x^{\mu}}{\mathrm{d}\tau}\frac{\mathrm{d}x^{\nu}}{\mathrm{d}\tau}=-1, \tag{10}$$

or

$$-\frac{\Delta}{r^2+a^2}\left(\frac{\mathrm{d}t}{\mathrm{d}\tau}\right)^2+\frac{r^2+a^2}{\Delta}\left(\frac{\mathrm{d}r}{\mathrm{d}\tau}\right)^2=-1. \tag{11}$$

Substituting Equation (9) yields

$$\left(\frac{\mathrm{d}r}{\mathrm{d}\tau}\right)^2=E^2-\frac{\Delta}{r^2+a^2}. \tag{12}$$

Our derivation applies to timelike test-particle geodesics and outward-moving trajectories. Massless particles are outside the scope of this work.

2.3.3. Transformation to Coordinate Time

Define

$$\dot{r}\equiv\frac{\mathrm{d}r}{\mathrm{d}t}.$$

Then

$$\dot{r}=\frac{\mathrm{d}r/\mathrm{d}\tau}{\mathrm{d}t/\mathrm{d}\tau}. \tag{13}$$

Differentiating with respect to t gives

$$\frac{\mathrm{d}^2r}{\mathrm{d}t^2}=\frac{1}{(\mathrm{d}t/\mathrm{d}\tau)^2}\left[\frac{\mathrm{d}^2r}{\mathrm{d}\tau^2}-\left(\frac{\mathrm{d}r}{\mathrm{d}\tau}\right)^2\frac{\mathrm{d}}{\mathrm{d}r}\ln\left(\frac{\mathrm{d}t}{\mathrm{d}\tau}\right)\right]. \tag{14}$$

From Equation (9),

$$\frac{\mathrm{d}}{\mathrm{d}r}\ln\left(\frac{\mathrm{d}t}{\mathrm{d}\tau}\right)=\frac{2r}{r^2+a^2}-\frac{2r-\alpha}{\Delta}=\frac{2r}{r^2+a^2}-\frac{2(r-\alpha/2)}{\Delta}. \tag{15}$$

A straightforward calculation using the proper-time radial equation then yields

$$\begin{aligned}\frac{\mathrm{d}^2r}{\mathrm{d}t^2}&=\left[\frac{2(r-\alpha/2)}{\Delta}-\frac{2r}{r^2+a^2}\right]\dot{r}^2\\&+\frac{\Delta^2}{E^2(r^2+a^2)^2}\left[-\frac{\alpha}{2}\frac{(r^2-a^2)}{(r^2+a^2)^2}+\frac{a^2(E^2-1)(3r^2-a^2)}{(r^2+a^2)^3}\right].\end{aligned} \tag{16}$$

This is the Kerr analogue of Equation (12) of [11].

2.3.4. Weak-Field Relativistic Limit

For $r\gg\alpha$ and $r\gg a$, Equation (16) becomes

$$\frac{\mathrm{d}^2r}{\mathrm{d}t^2}=\frac{\alpha}{r^2}\dot{r}^2-\frac{\alpha}{2E^2r^2}+\mathcal{O}\left(\frac{\alpha^2}{r^3},\frac{a^2}{r^4},\frac{\alpha a^2}{r^5}\right). \tag{17}$$

For relativistic motion,

$$\dot{r}^2 \simeq 1 - \frac{1}{E^2},$$

so that

$$\frac{\mathrm{d}^2 r}{\mathrm{d}t^2} = \frac{\alpha}{2r^2}\left(2 - \frac{3}{E^2}\right) + \mathcal{O}\left(\frac{\alpha^2}{r^3}, \frac{a^2}{r^4}, \frac{\alpha a^2}{r^5}\right). \tag{18}$$

Thus, for

$$E^2 > \frac{3}{2}, \tag{19}$$

the field is repulsive for distant observers. In the ultra-relativistic limit $E \gg 1$,

$$\frac{\mathrm{d}^2 r}{\mathrm{d}t^2} \approx \frac{\alpha}{r^2} = 2g, \quad g = \frac{GM}{r^2} = \frac{\alpha}{2r^2}. \tag{20}$$

The corresponding critical velocity condition is

$$\dot{r} > \frac{1}{\sqrt{2}E}. \tag{21}$$

2.3.5. Higher-Order Expansion and the Comparison with McGruder and Krori

Expanding Equation (16) to higher order, one obtains

$$\frac{\mathrm{d}^2 r}{\mathrm{d}t^2} = \frac{\alpha}{r^2} - \frac{\alpha^2}{r^3} + \frac{3a^2}{r^4} - \frac{4\alpha a^2}{r^4} + \mathcal{O}\left(\frac{\alpha^3}{r^4}, \frac{\alpha^2 a^2}{r^5}, \frac{a^4}{r^5}\right). \tag{22}$$

The individual terms in Equation (22) have distinct interpretations:

$$\frac{\alpha}{r^2} \quad \text{leading Schwarzschild term,} \tag{23}$$

$$-\frac{\alpha^2}{r^3} \quad \text{post-Newtonian mass correction,} \tag{24}$$

$$\frac{3a^2}{r^4} \quad \text{Boyer-Lindquist coordinate contribution,} \tag{25}$$

$$-\frac{4\alpha a^2}{r^4} \quad \text{genuine Kerr spin correction.} \tag{26}$$

At first sight, Equation (22) appears to differ from the results of [11] and [23], who obtain

$$a_D = +2g$$

for ultra-relativistic radial motion. There is, however, no contradiction. McGruder and Krori evaluate the exact geodesic expression for the radial coordinate acceleration and then take the asymptotic limit $r \to \infty$. By contrast, Equation (22) is a weak-field expansion of the same exact expression in powers of $1/r$.

Thus,

$$\lim_{r\to\infty} \frac{\mathrm{d}^2 r}{\mathrm{d}t^2} = \frac{\alpha}{r^2} = 2g, \tag{27}$$

while Equation (22) shows the subleading corrections that appear before the asymptotic limit is taken. The result $+2g$ is therefore the universal asymptotic behavior, whereas the additional terms in Equation (22) describe post-Newtonian and rotational corrections in the weak-field regime.

2.3.6. Graphical Comparison of Schwarzschild and Kerr Repulsion

To illustrate the effect of rotation, Figure 1 compares the weak-field ultra-relativistic Schwarzschild acceleration with the corresponding Kerr acceleration. For the Schwarzschild field we use

$$a_{\mathrm{S}}(r)=\frac{\alpha}{r^2}-\frac{\alpha^2}{r^3},$$

while for the Kerr field we use Equation (22),

$$a_{\mathrm{K}}(r)=\frac{\alpha}{r^2}-\frac{\alpha^2}{r^3}+\frac{3a^2}{r^4}-\frac{4\alpha a^2}{r^4}.$$

The plotted Kerr curve corresponds to the illustrative choice $a_*=a/M=0.95$. The two curves coincide asymptotically, where both reduce to the universal limit $a_D\to 2g$, but differ at smaller radii where the spin-dependent Kerr corrections become non-negligible.

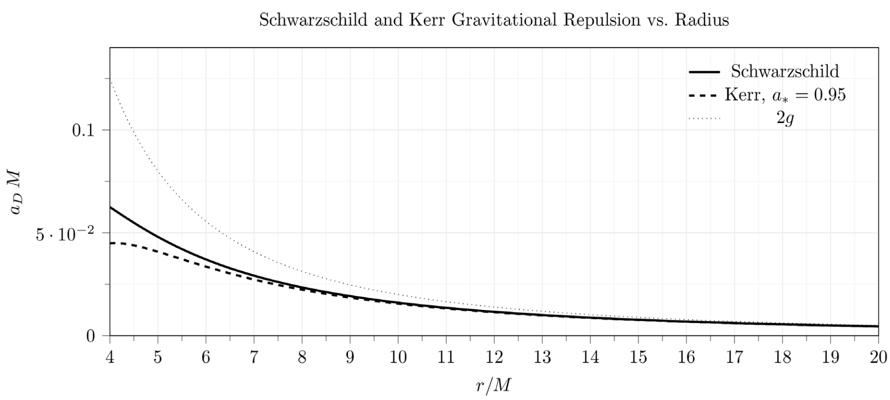

Figure 1. Comparison of the weak-field ultra-relativistic radial coordinate acceleration for the Schwarzschild and Kerr fields as a function of radius. Here $x=r/M$, and the vertical axis shows the dimensionless quantity $a_D M$. The Kerr curve uses the illustrative spin parameter $a_*=0.95$. At large radii the two curves approach the same asymptotic behavior, $a_D\to 2g$, while at smaller radii the Kerr spin corrections produce a visible deviation from the Schwarzschild result.

Note on Figure 1. Figure 1 corresponds to motion on the symmetry axis only, for which $\theta=0$, $L_z=0$, and $Q=0$. A separate graph for equatorial motion is not shown, since in the weak-field ultra-relativistic limit the equatorial acceleration has the same leading behavior,

$$\frac{\mathrm{d}^2r}{\mathrm{d}t^2}\approx\frac{\alpha}{r^2}=2g,$$

as the axial case. Differences between axial and equatorial motion appear only in the subleading rotational and coordinate-dependent terms.

2.4. Equatorial Motion

For motion in the equatorial plane, the leading weak-field result has the same form as Equation (18) for sufficiently energetic outward-moving particles. Thus the repulsive behavior persists away from the symmetry axis to leading order, although higher-order rotational corrections depend on the detailed geometry of the trajectory.

Relativistic Motion in the Equatorial Plane

We now consider motion in the equatorial plane: $\theta = \frac{\pi}{2}$ and $Q = 0$. Since frame dragging prevents motion from remaining strictly radial in the Schwarzschild sense, the closest equatorial analogue is obtained by taking: $L_z = 0$ so that the particle has zero conserved axial angular momentum even though its Boyer-Lindquist azimuthal motion need not vanish.

Define

$$\Delta = r^2 - \alpha r + a^2,\ C(r) = r^3 + a^2 r + \alpha a^2,\ \dot{r} = \frac{\mathrm{d}r}{\mathrm{d}t}.$$

Then

$$\begin{aligned} \frac{\mathrm{d}^2 r}{\mathrm{d}t^2} &= \left[\frac{1}{r} + \frac{2(r-\alpha/2)}{\Delta} - \frac{3r^2 + a^2}{C(r)}\right]\dot{r}^2 \\ &\quad + \frac{\Delta^2}{E^2 C(r)^2}\left[-\frac{\alpha}{2} + \frac{a^2(1-E^2)}{r} - \frac{3\alpha a^2 E^2}{2r^2}\right]. \end{aligned} \tag{28}$$

This is the equatorial Kerr analogue of Equation (16) for a particle with $L_z = 0$.

In the weak-field limit,

$$r \gg \alpha,\ r \gg a,$$

Equation (28) becomes

$$\frac{\mathrm{d}^2 r}{\mathrm{d}t^2} = \frac{\alpha}{r^2}\dot{r}^2 - \frac{\alpha}{2E^2 r^2} - \frac{a^2}{r^3}\left(1 - \frac{1}{E^2}\right) + O\left(\frac{\alpha^2}{r^3}, \frac{\alpha a^2}{r^4}, \frac{a^4}{r^5}\right). \tag{29}$$

The term proportional to a^2/r^3 is a Boyer-Lindquist coordinate effect, since even for $M = 0$ these coordinates reduce to oblate spheroidal coordinates in flat spacetime. Removing this flat-space contribution, the gravitational part of the weak-field acceleration becomes

$$\frac{\mathrm{d}^2 r}{\mathrm{d}t^2} = \frac{\alpha}{r^2}\dot{r}^2 - \frac{\alpha}{2E^2 r^2} + O\left(\frac{\alpha^2}{r^3}, \frac{\alpha a^2}{r^4}\right). \tag{30}$$

Hence

$$\frac{\mathrm{d}^2 r}{\mathrm{d}t^2} = \frac{\alpha}{2r^2}\left(2 - \frac{3}{E^2}\right) + O\left(\frac{\alpha^2}{r^3}, \frac{\alpha a^2}{r^4}\right), \tag{31}$$

and therefore, for $E \gg 1$,

$$\frac{\mathrm{d}^2 r}{\mathrm{d}t^2} \approx \frac{\alpha}{r^2} = 2g. \tag{32}$$

Thus the equatorial Kerr case gives the same leading relativistic repulsion for distant observers as the axial case.

The condition for repulsion is again: $\frac{\mathrm{d}^2 r}{\mathrm{d}t^2} > 0$, which yields

$$\dot{r} > \frac{1}{\sqrt{2}E}. \tag{33}$$

Thus, both on the axis and in the equatorial plane, the Kerr field is repulsive for distant observers when the outward-moving particle is sufficiently relativistic. To leading order,

$$\frac{\mathrm{d}^2 r}{\mathrm{d}t^2} \approx 2g,$$

and the critical velocity is determined by Equation (21) or Equation (33).

3. Astrophysical Implications

Ultra-high-energy cosmic rays and high-energy neutrinos provide observational evidence for particles with extreme relativistic energies [24]-[27]. For particles with

$$E^2 \gg \frac{3}{2},$$

the radial coordinate acceleration approaches

$$\frac{\mathrm{d}^2 r}{\mathrm{d}t^2} \approx 2g.$$

Relativistic particle production is believed to occur in environments such as active galactic nuclei, relativistic jets, and compact objects [5]. If the characteristic particle energy scales with source mass, then more massive sources naturally produce particles satisfying the repulsion condition.

Figure 2 illustrates schematically how a source-mass scaling of particle energy places ultra-relativistic particles well within the repulsive regime. This suggests that gravitational repulsion may contribute to the outward propagation of ultra-relativistic particles in astrophysical environments [12]-[14].

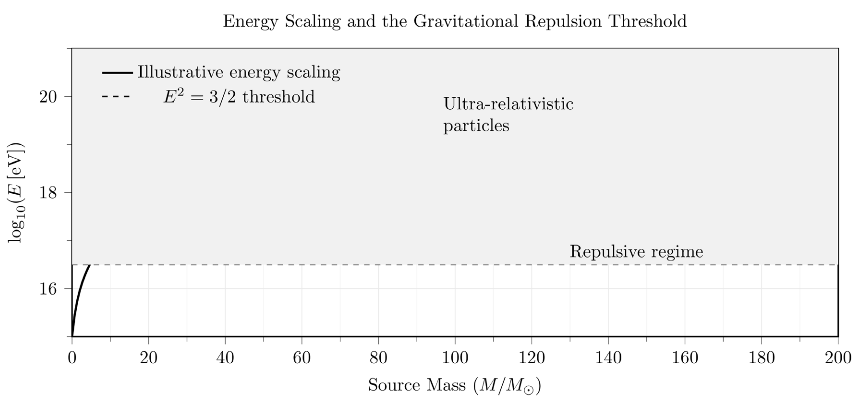

Figure 2. Illustrative particle energy as a function of source mass. The dashed horizontal line marks the threshold $E^2 = 3/2$, above which the radial coordinate acceleration becomes positive for distant observers. The shaded region indicates the repulsive regime. Ultra-high-energy particles lie well above this threshold.

3.1. Influence of Rotation: Astrophysical Examples

The Kerr metric provides an exact solution for the exterior spacetime of rotating black holes. For extended astrophysical bodies such as stars, brown dwarfs, and planetary objects, however, the exterior spacetime generally differs from the Kerr solution due to the presence of higher-order multipole moments and internal structure. In such cases, the Kerr metric should be regarded as an approximation that is valid in the exterior vacuum region sufficiently far from the source, where the spacetime is well approximated as stationary and axisymmetric and where deviations from the Kerr form enter as higher-order corrections. More precisely, deviations from the Kerr spacetime may be characterized by higher multipole moments beyond mass and angular momentum, which are not captured in the Kerr geometry.

Accordingly, the results derived here apply exactly to rotating black holes, while for stars, brown dwarfs, and planetary bodies they should be interpreted as approximate descriptions valid within this regime. The source-specific implications discussed below are therefore restricted to situations in which the Kerr approximation provides an adequate representation of the exterior gravitational field.

The rotation parameter a is given by

$$a = \frac{J}{M},$$

and is often expressed in dimensionless form as

$$a_* = \frac{a}{M} = \frac{J}{M^2}, \quad 0 \le a_* \le 1.$$

Astrophysical objects exhibit a wide range of spin parameters. Rapidly rotating black holes provide the largest known values of a. Observations indicate that stellar-mass black holes such as Cygnus X-1 and GRS 1915+105 [28] [29] have

$$a_* \approx 0.9 - 1,$$

while supermassive black holes in active galactic nuclei may also reach [30] [31]

$$a_* \gtrsim 0.9.$$

By contrast, neutron stars typically satisfy [32] [33]

$$a_* \lesssim 0.3,$$

and for stars and brown dwarfs one has [1] [34]

$$a_* \ll 1.$$

Thus the spin-dependent terms in Equation (17),

$$-\frac{4\alpha a^2}{r^4},$$

are expected to be significant primarily in the vicinity of rapidly rotating black holes.

For an extreme Kerr black hole with $a_* \approx 1$, one has $a \approx M$, and the spin correction scales as

$$\frac{\alpha a^2}{r^4} \sim \frac{M^3}{r^4}.$$

Relative to the leading term α/r^2, this gives

$$\frac{\text{spin correction}}{\text{leading term}} \sim \frac{M^2}{r^2}.$$

Thus rotational effects are most important close to compact objects, while at large distances the acceleration reduces to the universal form

$$\frac{d^2 r}{dt^2} \approx \frac{\alpha}{r^2} = 2g.$$

3.2. Connection to Astrophysical Acceleration Models

Gravitational repulsion in the Schwarzschild field has been invoked in the literature as a possible mechanism for accelerating ultra-high-energy particles [12]-[14]. In such approaches, the leading-order result

$$a_D = +2g$$

is used as the effective acceleration for relativistic motion as measured by distant observers.

The analysis presented here provides a more complete general-relativistic framework for such applications. In particular, we have shown that the result $+2g$ corresponds to the asymptotic limit of a more general expression for the radial coordinate acceleration, given in Equation (17). The additional terms in this expansion represent post-Newtonian mass corrections as well as spin-dependent contributions arising from the Kerr geometry.

Thus, while the leading-order behavior remains valid at large distances, Equation (17) demonstrates that corrections arise at finite radii. These corrections are especially relevant in the vicinity of compact objects, where higher-order and rotational effects cannot be neglected.

Furthermore, the extension from the Schwarzschild to the Kerr spacetime shows that gravitational repulsion is not restricted to non-rotating sources. Since astrophysical compact objects are generically rotating, the inclusion of Kerr terms is essential for a consistent description of particle dynamics in realistic environments.

Accordingly, the present results place gravitational repulsion-based acceleration mechanisms on a more general theoretical footing, while also delineating the regime in which the leading-order approximation is valid. In this sense, the commonly cited result $a_D = +2g$ represents a limiting case of a more general relativistic behavior.

3.3. Spin Magnitude: Fastest Neutron Star

For the fastest known neutron star, PSR J1748-2446ad, with spin frequency $f = 716\ \text{Hz}$ (period 1.396 ms) [35], one can estimate the dimensionless spin parameter

$$a_* \equiv \frac{cJ}{GM^2}, \ J \simeq I\Omega, \ \Omega = 2\pi f.$$

Taking a representative moment of inertia $I \simeq 1.4 \times 10^{45}\ \text{g} \cdot \text{cm}^2$ and $M \simeq 1.4 M_\odot$ [32] [33], one finds

$$a_* \sim 0.35 - 0.4.$$

Thus even the most rapidly rotating neutron stars are well below the near-extremal Kerr regime $a_* \sim 1$ characteristic of rapidly spinning black holes. Consequently, spin-dependent Kerr corrections in Equation (17) are expected to be most significant for black holes, whereas neutron stars provide a more modest contribution.

3.4. Spin Magnitude: Astrophysical Examples and Comparison Table

A concrete example of a rapidly rotating Kerr black hole is provided by Cygnus X-1, for which continuum-fitting analyses give

$$a_* > 0.95$$

[28]. Another near-extreme example is GRS 1915+105, for which

$$a_* > 0.98$$

has been reported [29]. For an illustrative near-extreme Kerr black hole with

$$a_* = 0.99,$$

one has

$$a = 0.99M.$$

Then the genuine spin-dependent correction in Equation (17) scales as

$$-\frac{4\alpha a^2}{r^4} = -\frac{4(2M)(0.99^2 M^2)}{r^4} \approx -\frac{7.84M^3}{r^4}.$$

Relative to the leading term

$$\frac{\alpha}{r^2} = \frac{2M}{r^2},$$

the ratio is

$$\frac{\left|-4\alpha a^2/r^4\right|}{\alpha/r^2} = \frac{4a^2}{r^2} \approx \frac{3.92M^2}{r^2}.$$

Thus, for a near-extreme Kerr black hole, spin corrections can be non-negligible in the near field, while remaining subleading at large radii.

For comparison, the fastest known neutron star, PSR J1748-2446ad, spins at 716.36 Hz (period 1.39595 ms) and is commonly estimated to have

$$a_* \sim 0.35 - 0.4$$

for representative masses and moments of inertia [35]. **Table 1** summarizes the approximate spin ranges relevant for the present discussion.

The comparison makes clear that the largest astrophysical Kerr corrections are expected for rapidly spinning black holes. Neutron stars provide an intermediate case, while ordinary stars and brown dwarfs are far from the relativistic Kerr regime.

Table 1. Representative dimensionless spin parameters $a_* = a/M$ for selected classes of astrophysical objects.

Object class	Example	Typical a_*
Brown dwarfs/stars	rapid rotators	$\ll 1$
Neutron stars	PSR J1748-2446ad	0.35 - 0.4
Stellar-mass black holes	Cygnus X-1	>0.95
Stellar-mass black holes	GRS 1915+105	>0.98
Near-extreme Kerr black hole	illustrative	0.99

4. Relation to Previous Work

The results obtained here are closely related to those of [11] and [23], who showed that the radial coordinate acceleration of ultra-relativistic particles in the Schwarzschild field [11] and the Kerr field [23] approaches

$$a_D = +2g$$

as observed by distant observers, where the gravitational field is weak.

In the present work, we have derived a weak-field expansion of the same quantity, given in Equation (17), which contains additional higher-order terms. These terms do not contradict the results of [11] and [23], but rather represent subleading corrections that vanish in the asymptotic limit $r \to \infty$.

Thus, the result $+2g$ corresponds to the universal asymptotic behavior, whereas Equation (17) provides a more detailed description of the acceleration at finite distances, including both post-Newtonian and spin-dependent Kerr contributions.

5. The Reality of Gravitational Repulsion

Observer dependence and local inertial measurements may be further clarified by contrasting the observer-at-infinity description adopted here with the measurements of local freely falling observers. In General Relativity, a freely falling observer follows a timelike geodesic and therefore measures zero proper acceleration, $a^\mu = u^\nu \nabla_\nu u^\mu = 0$. In this local inertial frame, the motion of a test particle is always consistent with free fall, and no repulsive force is detected in an invariant sense. By contrast, the quantity $\mathrm{d}^2 r/\mathrm{d}t^2$ considered in the present analysis is defined with respect to the coordinate time t of distant observers in an asymptotically flat spacetime, where t coincides with the proper time of inertial observers at infinity. Consequently, $\mathrm{d}^2 r/\mathrm{d}t^2$ represents the acceleration inferred by this specific class of observers and is therefore inherently coordinate-dependent, but not without physical content. Rather, it corresponds to an operationally well-defined measurement tied to a physically realizable observer family. This distinction between invariant local measurements and observer-dependent coordinate descriptions is standard in General Relativity (see, e.g., [1] [2]), and it underlies the interpretation of gravitational repulsion adopted in this work.

Gravitational repulsion has been the subject of considerable debate for over a century [11] [12]. Its very existence has often been questioned. For example, [36]-[39] maintain that Schwarzschild coordinates do not correspond to actual physical measurements, meaning the gravitational repulsion is simply a coordinate effect without physical reality.

In General Relativity, a distinction must be made between invariant quantities and coordinate-dependent quantities. Invariants, such as the spacetime interval $\mathrm{d}s^2$ or scalar curvature invariants, have the same value in all coordinate systems. By contrast, quantities such as $\mathrm{d}^2r/\mathrm{d}t^2$ depend on the choice of coordinates and therefore on the class of observers used to describe the motion. However, coordinate dependence does not imply lack of physical meaning; rather, it reflects the fact that different observers may assign different descriptions to the same physical trajectory.

The present work adopts the viewpoint of [11], in which gravitational repulsion is defined with respect to the coordinate time t of distant observers. This definition is physically meaningful because both the Schwarzschild and Kerr spacetimes are asymptotically flat. In the limit $r \to \infty$, the metric reduces to the Minkowski form, and the coordinate time t coincides with the proper time of inertial observers at infinity.

Thus, the radial coordinate acceleration, $\frac{\mathrm{d}^2r}{\mathrm{d}t^2}$, is naturally interpreted as the acceleration measured by distant observers in a weak-field region. In this sense, gravitational repulsion is not an arbitrary coordinate artifact, but a well-defined physical effect relative to a specific and physically realizable class of observers.

Accordingly, gravitational repulsion can be detected only by distant observers, for whom the time coordinate t has direct physical significance. This interpretation is consistent with the asymptotic structure of the spacetime and with the conserved energy $E = -p_t$, which represents the particle's relativistic energy as measured at infinity.

A central aim of this work is to clarify the physical interpretation of gravitational repulsion within the framework of General Relativity. Therefore we emphasize the fundamental issue and the response.

The key question is whether the coordinate acceleration $\mathrm{d}^2r/\mathrm{d}t^2$ at large distances represents a physically meaningful quantity or merely a coordinate artifact. The present analysis shows that, because Schwarzschild and Kerr spacetimes are asymptotically flat, the coordinate time t coincides with the proper time of inertial observers at infinity. Consequently, $\mathrm{d}^2r/\mathrm{d}t^2$ has a direct operational interpretation for these observers.

This interpretation provides a consistent general-relativistic framework within which gravitational repulsion arises naturally from the geodesic structure of spacetime, without the need for modifications of the theory.

6. Conclusion

We have extended the Droste and Hilbert analysis of gravitational repulsion in the Schwarzschild field to the Kerr field. We find that the repulsive behavior persists in rotating gravitational fields and that, for sufficiently energetic particles, the radial coordinate acceleration relative to distant observers becomes positive, that is gravity acts repulsively. The higher-order Kerr corrections separate naturally into post-Newtonian mass terms and genuine spin-dependent gravitational terms. These results suggest that gravitational repulsion may be relevant to the propagation of ultra-relativistic particles produced by astrophysical sources.

Acknowledgements

Many thanks to the family of Dr. and Mrs. William McCormick, whose generous support has provided the prerequisite financial basis and most importantly the necessary time to complete this project.

Conflicts of Interest

The author declares no conflicts of interest regarding the publication of this paper.

References

[1] Carroll, S.M. (2004) Spacetime and Geometry. An Introduction to General Relativity. Pearson Education (US).

[2] Misner, C.W., Thorne, K.S. and Wheeler, J.A. (1973) Gravitation. W. H. Freeman.

[3] Bardeen, J.M., Press, W.H. and Teukolsky, S.A. (1972) Rotating Black Holes: Locally Nonrotating Frames, Energy Extraction, and Scalar Synchrotron Radiation. *The Astrophysical Journal*, **178**, 347-370. https://doi.org/10.1086/151796

[4] Chandrasekhar, S. (1983) The Mathematical Theory of Black Holes. In: *General Relativity and Gravitation*, Springer, 5-26. https://doi.org/10.1007/978-94-009-6469-3_2

[5] Blandford, R.D. and Znajek, R.L. (1977) Electromagnetic Extraction of Energy from Kerr Black Holes. *Monthly Notices of the Royal Astronomical Society*, **179**, 433-456. https://doi.org/10.1093/mnras/179.3.433

[6] Droste, J. (1915) On the Field of a Single Centre in Einstein's Theory of Gravitation. *Proceedings of the Koninklijke Nederlandse Akademie van Wetenschappen*, *Series B*, *Physical Sciences*, **17**, 998-1011.

[7] Droste, J. (1917) The Field of a Single Centre in Einstein's Theory of Gravitation, and the Motion of a Particle in That Field. *Proceedings of the Royal Netherlands Academy of Arts and Sciences*, **19**, 197-215. https://www.lorentz.leidenuniv.nl/IL-publications/dissertations/biographies/Droste.pdf

[8] Hilbert, D. (1916) Die Feldgleichungen der Gravitation. Nachrichten von der Gesellschaft der Wissenschaften zu Göttingen, Mathematisch-Physikalische Klasse.

[9] Hilbert, D. (1917) Die Grundlagen der Physik (Zweite Mitteilung). In: *Nachrichten von der Gesellschaft der Wissenschaften zu Göttingen*, *Mathematisch-Physikalische Klasse*, Vandenhoeck & Ruprecht, 53-76.

[10] McGruder III, C.H. and Van Der Meer, B.W. (2018) The 1916 PhD Thesis of Johan-

nes Droste and the Discovery of Gravitational Repulsion. https://doi.org/10.48550/arXiv.1801.07592

[11] McGruder, C.H. (1982) Gravitational Repulsion in the Schwarzschild Field. *Physical Review D*, **25**, 3191-3194. https://doi.org/10.1103/physrevd.25.3191

[12] McGruder, C.H. (2017) Acceleration of Particles to High Energy via Gravitational Repulsion in the Schwarzschild Field. *Astroparticle Physics*, **86**, 18-20. https://doi.org/10.1016/j.astropartphys.2016.10.003

[13] McGruder III, C.H. (2026) The Cosmic Origin of High Energy Neutrinos, Ultra High Energy Neutrinos and the Mass of the Muon Neutrino. *Journal of Modern Physics*, **17**, 179-198. https://doi.org/10.4236/jmp.2026.172013

[14] McGruder III, C.H. (2026) Sources of Very High and Ultra High Energy Cosmic Ray Protons. *Journal of Modern Physics*, **17**, 483-505. https://doi.org/10.4236/jmp.2026.174022

[15] Krori, K.D., Sarmah, J.C. and Goswami, D. (1984) Gravitational Repulsion in the Einstein-Zero-Mass Scalar Theory. *Canadian Journal of Physics*, **62**, 629-631. https://doi.org/10.1139/p84-085

[16] Bragança, D.P.L. (2024) Gravitational Repulsion in an Expanding Ball of Dust. *Classical and Quantum Gravity*, **41**, Article 075008. https://doi.org/10.1088/1361-6382/ad2d70

[17] Polo, C.L. and Singh, H.S. (2024) Hilbert Repulsion in the Kerr-Newman Anti-De Sitter Spacetime. *Astrophysics and Space Science*, **369**, Article No. 41. https://doi.org/10.1007/s10509-024-04304-8

[18] Celerier, M.N., Santos, N.O. and Satheeshkumar, V.H. (2017) Hilbert Repulsion in the Reissner-Nordstrom and Schwarzschild Spacetimes. https://doi.org/10.48550/arXiv.1707.06994

[19] Gorkavyi, N. and Vasilkov, A. (2016) A Repulsive Force in the Einstein Theory. *Monthly Notices of the Royal Astronomical Society*, **461**, 2929-2933. https://doi.org/10.1093/mnras/stw1517

[20] Kutschera, M. and Zajiczek, W. (2009) Shapiro Effect for Relativistic Particles—Testing General Relativity in a New Window. https://doi.org/10.48550/arXiv.0906.5088

[21] Herrera, L. (2005) Geodesics in a Quash-Spherical Spacetime: A Case of Gravitational Repulsion. *Foundations of Physics Letters*, **18**, 21-36. https://doi.org/10.1007/s10702-005-2467-7

[22] Ponce de Leon, J. (1988) Gravitational Repulsion in Sources of the Reissner–Nordström Field. *Journal of Mathematical Physics*, **29**, 197-206. https://doi.org/10.1063/1.528172

[23] Krori, K.D. and Barua, M. (1985) Gravitational Repulsion by Kerr and Kerr-Newman Black Holes. *Physical Review D*, **31**, 3135-3139. https://doi.org/10.1103/physrevd.31.3135

[24] Pierre Auger Collaboration (2017) Observation of a Large-Scale Anisotropy in the Arrival Directions of Cosmic Rays above 8×10^{18} eV. *Science*, **357**, 1266-1270.

[25] Abbasi, R.U., Abe, M., Abu-Zayyad, T., Allen, M., Azuma, R., Barcikowski, E., *et al.* (2018) Depth of Ultra High Energy Cosmic Ray Induced Air Shower Maxima Measured by the Telescope Array Black Rock and Long Ridge FADC Fluorescence Detectors and Surface Array in Hybrid Mode. *The Astrophysical Journal*, **858**, 76. https://doi.org/10.3847/1538-4357/aabad7

[26] Aartsen, M.G. (2018) Multi-Messenger Observations of a Flaring Blazar Coincident

with High-Energy Neutrino IceCube-170922A. *Science*, **361**, eaat1378.

[27] IceCube Collaboration (2018) Neutrino Emission from the Direction of TXS 0506+056 Prior to the IceCube-170922A Alert. *Science*, **361**, 147-151.

[28] Gou, L., McClintock, J.E., Reid, M.J., Orosz, J.A., Steiner, J.F., Narayan, R., *et al.* (2011) The Extreme Spin of the Black Hole in CYGNUS X-1. *The Astrophysical Journal*, **742**, 85. https://doi.org/10.1088/0004-637x/742/2/85

[29] McClintock, J.E., Shafee, R., Narayan, R., Remillard, R.A., Davis, S.W. and Li, L. (2006) The Spin of the Near-Extreme Kerr Black Hole GRS 1915+105. *The Astrophysical Journal*, **652**, 518-539. https://doi.org/10.1086/508457

[30] Reynolds, C.S. (2014) Measuring Black Hole Spin Using X-Ray Reflection Spectroscopy. *Space Science Reviews*, **183**, 277-294. https://doi.org/10.1007/s11214-013-0006-6

[31] Brenneman, L. (2013) Measuring the Angular Momentum of Supermassive Black Holes. https://doi.org/10.1007/978-1-4614-7771-6

[32] Lattimer, J.M. and Schutz, B.F. (2005) Constraining the Equation of State with Moment of Inertia Measurements. *The Astrophysical Journal*, **629**, 979-984. https://doi.org/10.1086/431543

[33] Lattimer, J.M. and Prakash, M. (2016) The Equation of State of Hot, Dense Matter and Neutron Stars. *Physics Reports*, **621**, 127-164. https://doi.org/10.1016/j.physrep.2015.12.005

[34] Shapiro, S.L. and Teukolsky, S.A. (1983) Black Holes, White Dwarfs, and Neutron Stars. Wiley. https://doi.org/10.1002/9783527617661

[35] Hessels, J.W.T., Ransom, S.M., Stairs, I.H., Freire, P.C.C., Kaspi, V.M. and Camilo, F. (2006) A Radio Pulsar Spinning at 716 Hz. *Science*, **311**, 1901-1904. https://doi.org/10.1126/science.1123430

[36] Spallicci, A.D.A.M. (2017) Comment on Acceleration of Particles to High Energy via Gravitational Repulsion in the Schwarzschild Field. *Astroparticle Physics*, **94**, 42-43.

[37] Boonserm, P., Ngampitipan, T. and Visser, M. (2018) Near-Horizon Geodesics for Astrophysical and Idealised Black Holes: Coordinate Velocity and Coordinate Acceleration. *Universe*, **4**, Article 68. https://doi.org/10.3390/universe4060068

[38] Deriglazov, A.A., Guzmán Ramírez, W. and Rojas, P. (2019) Comment on "Acceleration of Particles to High Energy via Gravitational Repulsion in the Schwarzschild Field" by C.H. Mcgruder III. *Astroparticle Physics*, **107**, 35-37. https://doi.org/10.1016/j.astropartphys.2018.12.001

[39] Grøn, Ø. (2018) No Gravitational Repulsion in the Schwarzschild Spacetime. *Astroparticle Physics*, **102**, 95-97. https://doi.org/10.1016/j.astropartphys.2018.05.006

Appendix

A. Intermediate Steps in the Derivation of the Coordinate-Time Acceleration

We provide intermediate algebra connecting conserved quantities to Equations (16) and (28).

A.1. Transformation

$$\frac{\mathrm{d}^2 r}{\mathrm{d}t^2} = \frac{1}{\left(\mathrm{d}t/\mathrm{d}\tau\right)^2}\left[\frac{\mathrm{d}^2 r}{\mathrm{d}\tau^2} - \left(\frac{\mathrm{d}r}{\mathrm{d}\tau}\right)^2 \frac{\mathrm{d}}{\mathrm{d}r}\ln\left(\frac{\mathrm{d}t}{\mathrm{d}\tau}\right)\right]. \quad (34)$$

A.2. Axial Case

$$\frac{\mathrm{d}^2 r}{\mathrm{d}\tau^2} = -\frac{1}{2}\frac{\mathrm{d}}{\mathrm{d}r}\left(\frac{\Delta}{r^2 + a^2}\right). \quad (35)$$

Substitution yields Equation (16).

A.3. Equatorial Case

$$\frac{\mathrm{d}^2 r}{\mathrm{d}\tau^2} = -\frac{1}{2}\frac{\mathrm{d}}{\mathrm{d}r}\left(\frac{\Delta}{C(r)}\right). \quad (36)$$

Substitution yields Equation (28).